

Challenges in Rapid Ground Motion Estimation for the Prompt Assessment of Global Urban Earthquakes

David J. Wald¹⁾, Paul S. Earle¹⁾, Kuo-Wan Lin¹⁾, Vincent Quitoriano¹⁾ and Bruce Worden²⁾

¹⁾U.S. Geological Survey, National Earthquake Information Center, Golden, Colorado

²⁾U.S. Geological Survey, Pasadena, California

Abstract

We discuss the use of ShakeMap for the rapid evaluation of shaking hazards of all significant earthquakes around the globe. This global ShakeMap is used in a new U.S. Geological Survey system referred to as PAGER, for the Prompt Assessment of Global Earthquakes for Response. PAGER is an automated alarm system, currently in prototype operation. This is being further developed to rapidly and accurately assess the severity of damage caused by an earthquake and to provide emergency relief organizations, government agencies, and the media with an estimate of the societal impact from the potential catastrophe. Although the global ShakeMaps used for PAGER are constrained in part by rapidly gathered ground motion and intensity data via the Internet and with rupture dimensions resolved with automated finite fault analyses, they are fundamentally predictive, relying on our best efforts at rapidly estimating ground motions. Such a task requires adaptation of a number of seismological tools that we discuss herein. These include the estimation of site amplification on a global basis, the automatic inclusion of strong motion data and macroseismic intensities, incorporating rupture finiteness (mainly rupture dimensions) derived from source modeling, and empirically predicting regionally specific ground motion amplitudes with corresponding instrumental intensities. Since the uncertainties the shaking hazard estimates map into uncertainties in our rapid loss estimates, we also discuss efforts to quantify the ShakeMap uncertainty as a function of spatial location on the map grid.

Key words : Prompts Assessment of Global Earthquakes, strong ground motions, earthquake damage

1. Introduction

We use predictive, or composite ShakeMaps (Wald *et al.*, 2005a) for the rapid evaluation of significant earthquakes globally in our new system referred to as PAGER, for Prompt Assessment of Global Earthquakes for Response (Earle and Wald, 2005). The U.S. Geological Survey (USGS) National Earthquake Information Center (NEIC) is developing this automated system to estimate overall impact immediately following global earthquakes. PAGER will notify personnel and provide important information to help emergency relief organizations, government agencies, and the media plan their response to earthquake disasters through alarms via pager, mobile phone, and e-mail. Alarms will include a concise

estimate of impact : red for severe, yellow for moderate, and green for little or no impact. The alarms will also report an estimate of the number of people exposed to varying levels of shaking, an estimate of the likely range of casualties and losses, and a measure of confidence in the system's impact assessment. Associated maps, including shaking distribution, population density, and susceptibility to landslides will be posted on the Internet. The basic flow and processing of information through PAGER is straightforward. However, the implementation—the science behind the system, the gathering of the necessary data sets, testing, and calibration—requires significant system development.

At the heart of the impact assessment system are

* e-mail: wald@usgs.gov

the timely and accurate earthquake locations and magnitudes that the USGS has been producing for decades. PAGER then uses these earthquake solutions to estimate the distribution ground shaking for any earthquake, of magnitude 5.5 or larger, using the methodology and software developed for ShakeMap (Wald *et al.*, 1999a). Global ShakeMaps (see <http://earthquake.usgs.gov/shake/global/shake>) are constrained by whatever data are available at the time, and they are continually updated as more data are received. Initially, a point source approximation (hypocenter and magnitude) is used to constrain region-specific empirical ground motion estimations and site amplification is approximated from the topographic gradient and elevation (Wald and Allen, 2007).

Additional constraints for these predictive maps come primarily from three important sources, the availability of which varies depending on the region in which the earthquake occurred, as well as a function of time after the earthquake occurrence. These constraints include: (1) additional earthquake source information, particularly fault rupture dimensions, (2) observed macroseismic intensities (provided via the USGS “Did You Feel It?” system, Wald *et al.*, 1999b; Wald *et al.* 2005b), and (3) observed ground motions available for near-source strong ground motion stations, where and when available.

For all ground motion estimates, uncertainty measures are critical for evaluating the range of possible losses, and allows users to gauge the appropriate level of confidence when using rapidly produced ShakeMaps as part of their post-earthquake critical decision making process. For this reason, computation of uncertainty and ongoing challenges in adequately quantifying it on a spatial grid are also discussed.

2. Ground Motion Prediction Challenges

At its essence, ShakeMap produces separate maps of ground motion shaking, including estimated intensity, peak ground acceleration and velocity, and peak spectral acceleration values over the area affected by significant shaking. More technical and scientific details are provided in the ShakeMap Manual (Wald *et al.*, 2005a). Importantly, associated with these maps of ground shaking are the underlying geographic (latitude/longitude) grids for each ground motion parameter values, which can be used by oth-

ers for additional purposes, for example, as input into loss estimation routines, or to evaluate the shaking at individual facilities or at many locations within an inventory portfolio. Corresponding Geographic Information Systems (GIS) shapefiles for each shaking parameter are also provided.

However, in order to infer ground shaking on a worldwide basis, several new ShakeMap approaches need to be taken that were not fully explored in the original ShakeMap system development. Likewise, more emphasis is made on constraining and inferring the earthquake source in order to better predict ground motions, as well as in quantifying the uncertainties associated with both these source and shaking inferences. We outline these new approaches and ongoing challenges to implementing them below.

2.1 Regional Ground Motion Prediction Equations

Calculation of ground shaking estimates for global earthquakes are initially based on a point-source approximation and empirical ground-motion prediction equations. From the earthquake’s location we assign region-specified, configuration parameters for ShakeMap (as well as others for loss estimation). Initially, ground motion prediction equations for active-tectonic, cratonic, subduction (both inter- and intra-slab), and extensional regimes are assigned automatically, but we will switch to more localized county-based assignment, as more relations are included. Rule-based configurations provide logic for choosing the appropriate relation, for example, hypocentral depth bounds define whether a crustal, intra-slab, or interslab relation is used.

We are also developing regional modifications to the existing ShakeMap instrumental intensity relationships, but this is an onerous task since infrastructure vulnerability, as well as ground motion and macroseismic intensity data availability, vary considerably from region to region. Currently, instrumentally derived intensity relations are only directly applicable to Japan, the western U.S. and the eastern U.S.

2.2 Site Amplification

Typically, maps of seismic site conditions on regional scales are difficult to come by since they require substantial investment in geological and geophysical data acquisition and interpretation. Such maps are available for only a few limited subsets of seismically active urban areas of the world, most notably for all of California and Japan (see Wills *et*

al., 2000 and Matsuoka *et al.*, 2005, respectively). Topographic elevation data, on the other hand, are available at uniform sampling globally, and we now derive site condition maps directly from the global topographic slope based on the approach of Wald and Allen (2007).

Intuitively, topographic variations should be an obvious indicator of regions of rock (mountains) and soil (basins) to first order. In fact, the overall similarities of topographic and surficial geologic maps where both are available assures that a site map based on divisions of topographic slope will independently recover at least the dominant features of the geology map. Since site conditions, and thus site amplifications, can be approximated from the surficial geology, this can be useful for first order site corrections.

For calibration, we used the California statewide topographic data and geologically-based shallow (30 m) site condition map and shear-wave values of Wills *et al.* (2000). By taking the gradient of the topography and choosing the ranges of slope that maximize the correlation with 30-m shear-velocity (V_{s30}) observations we can recover, to first order, many of the spatially varying features of the site-condition map for California (Figure 2). In addition to topographic gradient alone, we assign class E (bay mud) to all flat regions with elevations between plus and minus 3 meters. This assumption produces reasonable class E boundaries along nearly flat coastal regions that tend to be associated with very low V_{s30} values (see Figure 3). Using the same parameterization also recovers many of the details of the site condition map for Japan developed by Matsuoka *et al.* (2005) in which they considered topography as well as detailed geomorphological classifications for their nationwide V_{s30} assignments.

The largest discrepancy in geologically- and topographically-derived site conditions is between soft and hard rock and the separation between these is made difficult for these units by the lack of shear-wave measurements for making statistically significant correlations with topographic slope as well as their comparable slope values. Fortunately, corresponding differences in site amplification inferred for these two different site classes are relatively small so our approximation holds.

As part of the ShakeMap generation process in which we overlay shaking on topography, we al-

ready compute the topographic gradient for our base map; the slope ranges and mean values are therefore already at hand. Ironically, we settled on using topography for ShakeMap base maps, since they tend to highlight areas of amplified shaking in basins from those less amplified mountainous areas. An unanticipated benefit of these base maps is for actually constraining the site factors directly. The topographic gradients can then be easily converted to NEHRP site amplification factors for estimating ground motions in direct conjunction with standard empirical ground motion prediction equations and can be used on a global basis (although more detailed site-condition maps can be locally substituted where available). Finally, we are investigating further the benefits of using topographic elevation in conjunction with slope as a proxy to site conditions, a correlative found to be beneficial in analyses by Matsuoka *et al.* (2005).

2.3 Incorporating Direct Observations

The USGS now has in operation a rapid and automatic web-based collection of intensity data, a global extension of the USGS “Did You Feel It?” web site (see Wald *et al.*, 2005b). Utilizing macroseismic intensities for ShakeMap is accomplished using the intensity values directly and by converting decimal Community Internet Intensity (CII, Wald *et al.*, 1999b) values into peak ground motions via the inverse of the ground motion versus intensity relationships of Wald *et al.* (1999c). This is exactly the opposite approach used in the standard ShakeMap instrumental intensity maps for which ground motions are related to color-coded intensities via the same relations. Again, the inverse relationship between observed intensities and ground motions will be regionally dependent as well, and thus these await development of instrumental intensity verses peak ground motions for other areas.

In some areas of the world where shaking maps are not produced, there are nonetheless some rapid strong motion data are available rapidly after an earthquake (via the World Wide Web), and in rural regions of the U.S. outside of regional networks (via rapid dialup). These data can be included as direct observations as in a standard ShakeMap and serve to correct any magnitude-based or inter-event bias in the ground motion prediction relation used.

In order to make best use of these varied data

ALERT	DATE	TIME	LAT	LOE	DEPTH	EXPOSURE	LOCATION
HTML_V2 PDF_V2	0.0	20050807 18:38:19	6.882	82.289	10.0	2,170,000 191,000	121 miles S of Davao, Panama
HTML_V1 PDF_V1	0.6	20050807 10:57:48	6.591	126.876	64.8	1,200 342,000	48 miles SE of General Santos, Mindanao, Philippines
HTML_V3 PDF_V3	6.2	20050809 18:16:33	16.483	122.286	10	17,000	148 miles NW of Galathea, Socotra Island, Yemen
HTML_V4 PDF_V4	6.9	20050804 10:14:49	38.501	143.086	29.2	9,200,000 794,000	120 miles E of Sendai, Honshu, Japan
HTML_V1 PDF_V1	6.7	20050804 17:07:46	10.121	103.909	10.0	No population exposure	100 miles E of Cebu, Cebu Island
HTML_V3 PDF_V3	6.2	20050804 10:16:30	38.471	142.836	50	3,140,000 285,000	68 miles E of Sendai, Honshu, Japan
HTML_V1 PDF_V1	6.5	20050819 10:48:19	2.021	126.076	81.8	112,000 285,000	135 miles SW of Tawale, Moluccas, Indonesia
HTML_V2 PDF_V2	6.0	20050814 07:38:51	20.151	165.786	40.8	No population exposure	138 miles N of Pagan, Northern Mariana Islands
HTML_V2 PDF_V2	6.9	20050814 02:39:40	19.758	68.800	113.6	23,000 394,000 1,380,000 1,160,000	67 miles ESE of Iquique, Chile
HTML_V1 PDF_V1	7.2	20050816 02:48:30	38.271	141.896	82.8	277,000 2,810,000 12,640,000 32,300,000	60 miles E of Sendai, Honshu, Japan
HTML_V1 PDF_V1	6.7	20050811 11:50:51	21.872	170.286	10.0	142,000 14,000	140 miles SSE of Nagasaki, Yamaguchi
HTML_V8 PDF_V8	6.1	20050809 02:28:21	21.088	172.656	49.8	No population exposure	104 miles SSE of Nagasaki, Yamaguchi

Fig. 1. PAGER event page, showing recent earthquakes as well as links to short reports. This list is served on <http://earthquake.usgs.gov/pager/alert> but requires a password to access (contact authors).

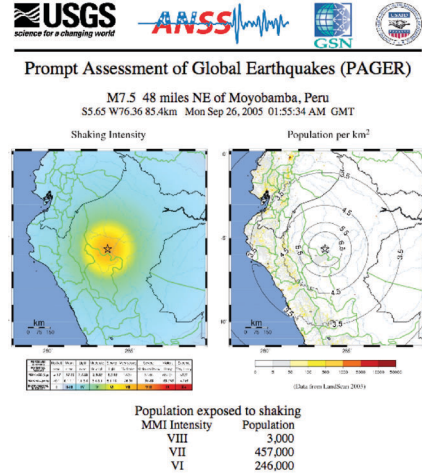


Fig. 2. PAGER short report summarizing the estimated shaking intensity distribution, population distribution, and population exposed to shaking.

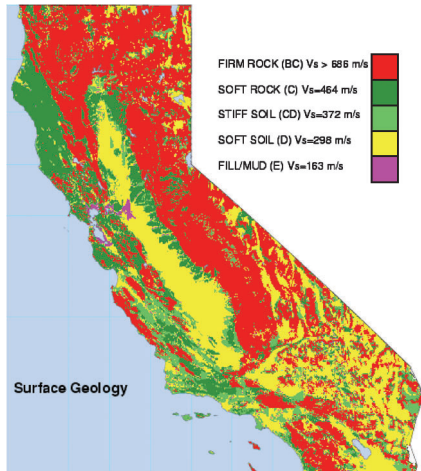


Fig. 3a. Site-condition map for California based on Geology and shear-wave velocity observations (modified from Wills et al., 2000).

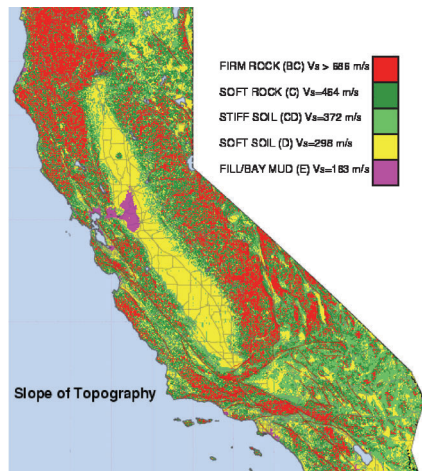


Fig. 3b. Site-condition map for California based on topographic slope alone (Wald and Allen, 2007).

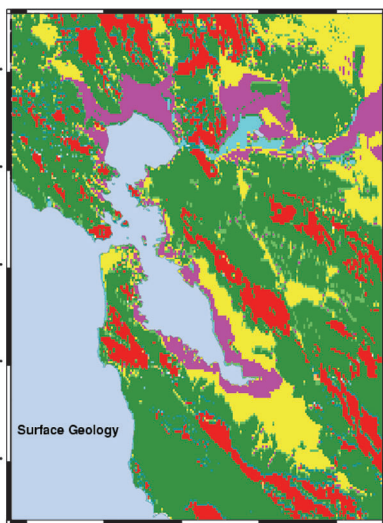


Fig. 4a. Site-conditions map for the San Francisco, California, bay area based on geology and shear-wave velocity observations (modified from Wills et al., 2000). Color scheme is the same as Fig. 3.

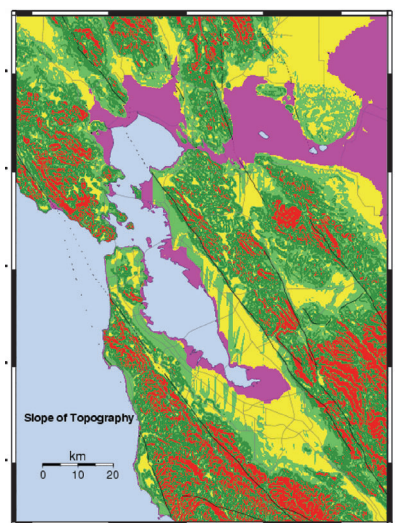


Fig. 4b. Site-conditions maps for the San Francisco, California, bay area based on topographic slope scheme of Wald and Allen (2007). Color scheme is the same as Fig. 3.

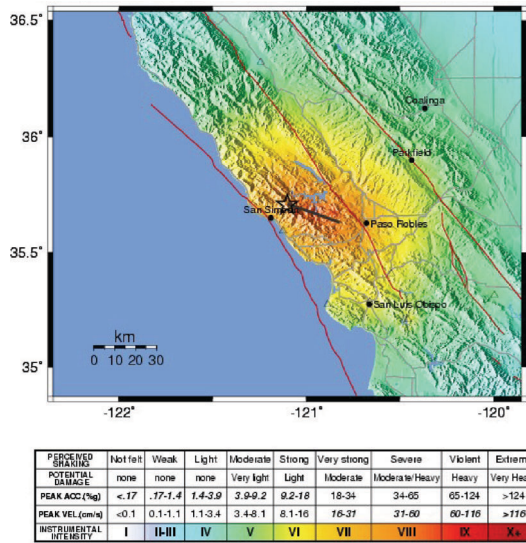


Fig. 5a. Magnitude 6.5 2003 San Simeon, California earthquake ShakeMap with fault finiteness imposed (line source shown as a grey line). Note there are few seismic stations in this region of California.

sets along with predicted peak ground motion values however, ShakeMap must allow prioritization of “data” in the following order (1) observed Intensities, (2) recorded Ground Motions, (3) numerical ground motions, (4) empirical ground motions. Further, an interesting challenge is in directly combining macroseismic and ground motion data. The former is less reliable but more directly applicable to the intensity maps, but they must be related to PGA and PGV to be used in peak motions maps ; the latter are more accurate, but must be related to the intensity for use in intensity maps. How co-located observations are to be used is still an open question, but we will likely assign specific parameters to specific map types preferentially.

2.4 Fault Finiteness

For very large (approximately magnitude 7.0 and larger) events, aftershock and finite fault analyses are also performed as rapidly as possible to determine the faulting geometry. The rupture dimension can be extremely important for improving empirically-based ground motion predictions, since it provides a more reasonable measurement of source-to-site distance used in the ground motion prediction equations. Knowledge of the rupture dimensions can dramatically improve the accuracy of the ground shaking estimates, as well as reduce the uncertainty in these estimates. We are currently developing and

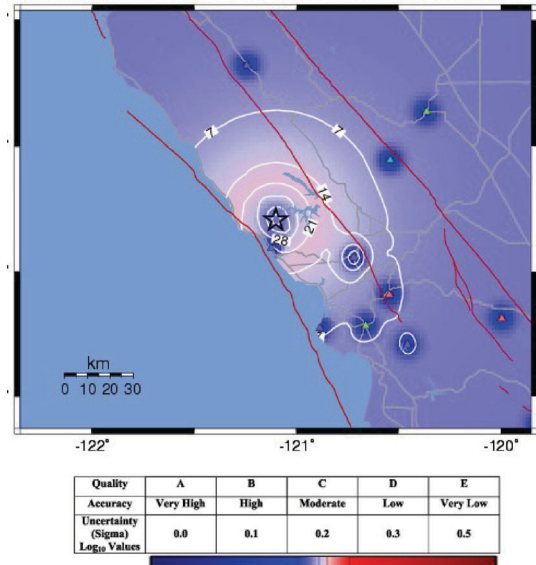


Fig. 5b. Uncertainty map, prior to adding finiteness,

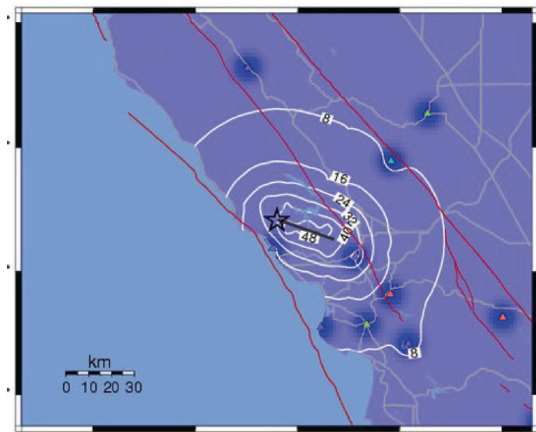


Fig. 5c. Uncertainty map, after adding finiteness. See Figure 5b for the color legend.

Likewise, in the U.S., PAGER estimates of impact will provide a rapid first cut indication of the likely impact of an earthquake. The Federal Emergency Management Agency (FEMA), as well as some state Emergency Services Offices, have the capability of computing losses based on ShakeMap input with FEMA’s Hazard’s U.S. (HAZUS) loss estimation software. HAZUS-based loss estimates are based on more extensive structure and census inventories and have more rigorous loss estimation methodologies than does the prototype PAGER system, and thus they will have precedence over PAGER estimates. PAGER is still in the early stages of development but is progressing towards a fast and accurate system that international and domestic users can rely on. The PAGER team is continuously seeking collaboration with other agencies, domestic and worldwide, to create a system that will benefit both the system users and the populations of earthquake stricken areas.

implementing automated finite fault inversions (e.g., Ji *et al.*, 2004) at the USGS National Earthquake Information Center (NEIC).

In practice, after an event is located (now routinely less than 15 minutes globally), a moment tensor inversion (CMT) is automatically triggered at NEIC, which in turn triggers and provides input into the finite fault inversion. Both fault planes are examined, and the one returning the lower residual fit to the data is further modeled for slip heterogeneity (see Ji *et al.*, 2004). In theory, we can also use numerically-based estimates of ground motions from forward waveform modeling of the finite-fault rupture model for significant earthquakes, but this will require more research, validation, and implementation challenges.

In conjunction with fast finite-fault inversions, NEIC is also complementing the modeling with research and development of rapid aftershock identification tools and is prioritizing the association of aftershocks immediately after big earthquakes. A quick view of the aftershock distribution can provide confirmation of modeling results or can independently allow estimation of fault rupture dimensions.

2.5 Quantifying Ground Motion Uncertainty

The accuracy of a given ShakeMap, which varies spatially over the map area, depends on a number of contributing factors (Lin *et al.*, 2005). However, the uncertainty is usually dominated by two aspects : (1) spatial variability of peak ground motions near intensity observations or recording stations (and hence, observation density), and (2) the aleatory uncertainty associated with empirical ground motion estimation relations used to fill in station gaps. In this discussion, we focus on these two sources of variability in estimating ShakeMap uncertainty ; other secondary issues are also being analyzed. Spatial variability of peak ground motions can be generalized in the form of a rapidly increasing variability with increasing distance from the nearest station. Aleatory variability, in contrast, is more complicated and becomes more significant as the fault dimensions get larger (about M5.5 and greater), particularly when the fault location and dimensions are not yet ascertained. Without an accurate representation of the fault rupture geometry, the appropriate distance to a particular location—which is needed when using a forward ground motion prediction equation—is poorly con-

strained. Not knowing the true distance to the fault rupture contributes significant uncertainty, particularly in the near-fault region, and this uncertainty scales with magnitude.

Our goal in quantifying ShakeMap uncertainty is to produce a grid of latitude and longitude pairs that contain not only the various peak ground motion parameters at each point, but also contain the variance at that point for each ground motion parameter. This grid could also be converted to an overall *qualitative* assignment of ShakeMap accuracy, a challenge we will be addressing in the near future. In the meantime, for generating a map of ShakeMap uncertainty values at each grid point, we consider three end member cases.

1) Small to moderate sized earthquake, suitable for a point source representation

When a grid point is near a station (10 km or less), uncertainty is controlled by proximity to that station as defined by variability quantified by Boore *et al.* (2003)

$$\sigma_{\Delta \log Y}^2 = \sigma_{indobs}^2 \left(1 + \frac{1}{N}\right) F(\Delta)^2 \text{ and} \\ F = 1 - e^{-\sqrt{0.6\Delta}} \quad (1)$$

where $\sigma_{\Delta \log Y}$ is the standard deviation of differences in the logarithm of the peak motion Y , σ_{indobs} is the standard deviation of an individual observation about a regression, and N is the number of recordings used in the average of a group of recordings in a small region. $f(\Delta)$ is a function that accounts for spatial correlation of the motion, where Δ is the distance between the sites. For this study we assumed that N is enough large so that the $1/N$ term can be neglected. Thus, the spatial variability in ground motion reduces to zero as the distance between a grid point and the nearest station decreases to zero (see Figure A1 in the Appendix of Boore *et al.*, 2003). With a large grid point to station distance, the spatial variability in ground motion approaches the standard deviation of the regression model. The cut-off distance for computing spatial variability in ground motion is set at 10 km in our study. For greater distances, we use the total aleatory uncertainty (sigma) of Boore *et al.* (1997) ground motion prediction equations :

$$\sigma_{Aleatory} = \sqrt{\sigma_{Interevent}^2 + \sigma_{Intraevent}^2} \quad (2)$$

With several ShakeMap data points (station amplitudes), we can remove a bias term between the forward ground motion predictions and the data, thereby removing the inter-event term. However, when no data are available, no event-specific bias correction can be made and both the intra- and inter-event terms contribute (Equation 2).

2) Large earthquake, where fault rupture geometry and dimensions are not known

For earthquakes of magnitude 5.5 and larger, the fault dimension affects one's measure of the distance from the fault to the site of interest. When employing the Joyner-Boore distance measure used for forward ground motion estimation, the fault rupture dimension must be known. Recall that the Joyner-Boore distance is defined as the closest distance from a site to the surface projection of the fault rupture. If necessary, initial ShakeMaps are produced without knowledge of the rupture dimensions. Again, the uncertainty is generally low near the seismic stations, but at some distance from the stations it is constrained only by the forward predictions using a ground motion attenuation relation and knowledge of the site condition. In this case, distance adjustments are made to convert the point source (epicentral) distance used to the appropriate Joyner-Boore distance for the ground motion attenuation model used. We also must adjust the aleatory uncertainty. We adopt the results and the approach defined in EPRI (2003), in which the distance adjustment is determined for the case where the rupture orientation is assumed to be uniformly distributed in azimuth from 0 to 360 degrees and for a mixture of strike-slip and reverse ruptures using random epicenters. For each simulated rupture, EPRI (2003) :

- i) Computed the appropriate distance measure and corresponding median ground motion parameter,
- ii) Considered the geometric mean of all these simulation values to be the median ground motion for that epicentral distance and magnitude,
- iii) Inverted the median ground motion to find the distance that corresponds to that median ground motion value,
- iv) Determined a distance adjustment factor for each epicentral distance, magnitude, and ground motion parameter, and
- v) Fit these distance adjustment factors with a functional form, and provided the necessary co-

efficients in a series of look up tables.

Using the distance correction factor then simply entails employing these distance adjustment relationships (EPRI, 2003) that translate epicentral to the equivalent Joyner-Boore distance :

$$r_{\text{Joyner-Boore}} = r_{\text{Epicentral}} \times \{1 - 1/\cosh(C_1 + C_2(M-6) + C_3 \ln(r'))\} \quad (4)$$

$$\text{where } r' = \sqrt{r_{\text{Epicentral}}^2 + h^2} \quad (5)$$

$$h = e^{C_4 C_5 (M-6)} \quad (6)$$

$r_{\text{Joyner-Boore}}$ is the Joyner-Boore distance, $r_{\text{Epicentral}}$ is the epicentral distance, M is the magnitude of the earthquake, and $C1$ to $C5$ are the EPRI (2003) model coefficients (the coefficients vary by ground motion model and seismic frequency).

Hence, when the fault geometry and orientation is not known, a mean value of ground motion at each point is provided rather than the simple epicentral distance-based estimation. While the latter approach is currently used for ShakeMap, it tends to underestimate ground motions near a finite fault (since it is the maximum possible source-station distance) rather than providing a mean value based on random fault geometry and epicenter. Hence, we adopted these distance adjusted ground motions for ShakeMap production.

The variability associated with this approach is also derived in EPRI (2003). The variability in the median ground motion, due to the randomness in epicenter location and rupture orientation, was used to compute a ground motion standard deviation and we employ their equations to compute the additional component of aleatory uncertainty :

$$\sigma_{\text{Additional Point Source}} = e^{C_1 + C_2(M-6) + C_3(M-6)^2} \times [1 - 1/\cosh(f_a)] \times 1/\cosh(f_b) \quad (7)$$

$$f_a = e^{C_4 + C_5(M-6)} + e^{C_6 + C_7(M-6)} \times r_{\text{Epicentral}} \quad (8)$$

$$f_b = e^{C_8 + C_9(M-6)} \times \ln(r'/h), \quad (9)$$

$$r' = \sqrt{r_{\text{Epicentral}}^2 + h^2}, \quad h = e^{C_{10} + C_{11}(M-6)} \quad (10)$$

where $\sigma_{\text{Additional Point Source}}$ is the point source aleatory, $r_{\text{Epicentral}}$ is the epicentral distance, M is the magnitude of the earthquake, and $C1$ to $C11$ are the model coefficients given in the EPRI (2003). We can then combine this additional point source variability (Equation 7) with that associated with the prediction

equation (Equation 2) :

$$\sigma_{total} = \sqrt{\sigma_{Aleatory}^2 + \sigma_{Additional Point Source}^2} \quad (11)$$

An example of this uncertainty is shown in Figure 4b. Again, if at any time a grid point is closer to a station than 10 km, the variability associated with that grid to station distance controls the uncertainty and is thus lower ; at greater distances, the above relation is employed and the uncertainty can be significantly higher (see Figure 4b).

3) Large earthquake, where fault rupture geometry and dimensions are known

Here, the uncertainty is greatly reduced in comparison to the point source approximation as the site to source can be calculated correctly (see Figure 4c).

Currently, the uncertainty calculations are limited to the Boore *et al.* (1997) relationship and the Joyner-Boore distance measure ; this needs to be expanded to subduction zone rupture geometry uncertainty as well. Finally, another element of uncertainty that we need to determine and quantify is that of hypocentral location error (latitude, longitude, and depth), both for the point source approximation and as it pertains to the relative location of a finite fault model. For a regional network with small location errors, this can be ignored, but for teleseismic source locations globally errors can be on the order of 10 km.

3. Discussion

The same predictive tools developed for estimating shaking intensity distribution and loss estimation based on recorded earthquake parameters can also be utilized for generating ShakeMaps for earthquake scenarios and computing the potential losses from these scenarios. Examining the potential impact of selected earthquake scenarios can be fundamental for evaluating and focusing mitigation as well as for emergency response planning.

The global ShakeMap system will have different roles for earthquakes that occur within areas of the world that produce data-constrained shaking maps, including all of Japan, Taiwan, and those areas of the U.S. in which regional networks generate ShakeMaps (all of California, for example) than it will for events worldwide. In the U.S., some of the regions most at risk have ShakeMap systems that are well constrained by relatively dense ground motion recordings. Such data-rich maps will take precedence

over PAGER's estimated global ShakeMap approach, though the global ShakeMap system is also intended to provide fail-safe backup for the regional systems in case of catastrophic communications or other failures. Likewise, in the U.S., PAGER estimates of impact will provide a rapid first cut indication of the likely impact of an earthquake. The Federal Emergency Management Agency (FEMA), as well as some state Emergency Services Offices, have the capability of computing losses based on ShakeMap input with FEMA's Hazard's U.S. (HAZUS) loss estimation software. HAZUS-based loss estimates are based on more extensive structure and census inventories and have more rigorous loss estimation methodologies than does the prototype PAGER system, and thus they will have precedence over PAGER estimates.

PAGER is still in the early stages of development but is progressing towards a fast and accurate system that international and domestic users can rely on. The PAGER team is continuously seeking collaboration with other agencies, domestic and worldwide, to create a system that will benefit both the system users and the populations of earthquake stricken areas.

Acknowledgments

This workshop at which this paper was presented was sponsored by the Special Project for Earthquake Disaster Mitigation in Urban Areas from the Ministry of Education, Culture, Sports, Science and Technology of Japan.

References

- Boore, D.M., Gibbs, J.F., Joyner, W.B., Tinsley, J.C. and Ponti, D.J (2003). Estimated Ground Motion From the 1994 Northridge, California, Earthquake at the Site of the Interstate 10 and La Cienega Boulevard Bridge Collapse, West Los Angeles, California, *Bull. Seism. Soc. Am.*, **93**, 6, 2737-2751.
- Boore, D.M., W.B. Joyner and T.E. Fumal (1997). Equations for Estimating Horizontal Response Spectra and Peak Accelerations from Western North American Earthquakes : A Summary of Recent Work, *Seism. Res. Lett.*, **68**, 128-153.
- Earle, P.S. and D.J. Wald (2005). Helping Solve a Worldwide Problem—Rapidly Estimating the Impact of an Earthquake, U.S. *Geological Survey Fact Sheet* 2005-3026. <http://pubs.usgs.gov/fs/2005/3026/>
- EPRI (2003). CEUS Ground Motion Project : Model Development and Results, *EPRI Report 1008910*, EPRI, Palo Alto, CA.
- Ji, C, D.V. Helmberger and D.J. Wald (2004). A teleseismic

- study of the 2002, Denali, Alaska, earthquake and implications for rapid strong motion estimation, *Earthquake Spectra*, **20**, 617–637.
- Lin, K.W., D.J. Wald, B. Worden and A.F. Shakal (2005). Quantifying CISM ShakeMap Uncertainty, CSMIP'05 Seminar on the Utilization of Strong Motion Data, CSMIP User's Workshop, Proceedings, Los Angeles, CA., p. 37–49.
- Matsuoka, M., Wakamatsu, K. Fujimoto, K. and Midorikawa, S. (2005). Nationwide site amplification zoning using GIS-based Japan Engineering Geomorphologic Classification Map, *Safety and Reliability of Eng. Systems and Structures (Proc. 9th Inter. Conf. on Structural Safety and Reliability, Millpress*, CD-ROM, pp. 239–246.
- Wald, D.J., V. Quitoriano, T.H. Heaton, H. Kanamori, C.W. Scrivner and C.B. Worden (1999a). TriNet "ShakeMaps" : Rapid Generation of Peak Ground Motion and Intensity Maps for Earthquakes in Southern California, *Earthq. Spectra*, Vol. **15**, No. 3, 537–556.
- Wald, D.J., V. Quitoriano, L. Dengler and J.W. Dewey (1999 b). Utilization of the Internet for Rapid Community Intensity Maps, *Seism. Res. Letters*, **70**, No.6, 680–697.
- Wald, D.J., V. Quitoriano, T.H. Heaton and H. Kanamori (1999c). Relationship between Peak Ground Acceleration, Peak Ground Velocity, and Modified Mercalli Intensity for Earthquakes in California, *Earthquake Spectra*, Vol. **15**, No. 3, 557–564.
- Wald, D.J., B.C. Worden, V. Quitoriano and K.L. Pankow (2005a). ShakeMap Manual : Users Guide, Technical Manual, and Software Guide, USGS Techniques and Methods 12-A1, 128 pp. <http://pubs.usgs.gov/tm/2005/12A01/>
- Wald, D.J., V. Quitoriano and J.W. Dewey (2005b). Did You Feel It ?" Goes Global : Testing the USGS Community Internet Intensity Map (CIIM) Procedure for Non-U.S. Earthquakes, *Seismo. Res. Lett.* **76**, No. 2, p. 231
- Wald, D.J. and T. Allen (2007), Topographic Slope as a Proxy for Seismic Site Conditions and Amplification, submitted to *Bull. Seism. Soc. Am.*
- Wills, C.J., M.D. Petersen, W.A. Bryant, M.S. Reichle, G.J. Saucedo, S.S. Tan, G.C. Taylor and J.A. Treiman (2000). A site-conditions map for California based on geology and shear wave velocity, *Bull. Seism. Soc. Am.*, **90**, S187-S208.

Related World Wide Web URLs :

- PAGER Home Page :
<http://earthquake.usgs.gov/pager/>
- PAGER Impact Summaries (Password Required) :
<http://earthquake.usgs.gov/pager/alert/>
- ShakeMap (Global Events) :
<http://earthquake.usgs.gov/shakemap/global/shake/>
- USGS "Did You Feel It ? (Global Events) :
<http://pasadena.wr.usgs.gov/shake/ous/>

(Received November 2, 2005)

(Accepted March 3, 2006)